Electronic Supplementary Material (ESI) for CrystEngComm.

Crystallisation and physicochemical property characterisation of conformationally-locked co-crystals of fenamic acid derivatives

K. E. Wittering,[a,b] L. R. Agnew,[a,b] A. R. Klapwijk,[a,b] K. Robertson,[a,b] A. J. P. Cousen,[a,b] D. L. Cruickshank, *[a] and C. C. Wilson*[a]

[a] *Department of Chemistry, University of Bath, Bath, BA2 7AY*

[b] *Engineering and Physical Sciences Research Council (EPSRC) Centre for Innovative Manufacturing in Continuous Manufacturing and Crystallisation (CMAC), University of Bath, Bath, BA2 7AY*

c.c.wilson@bath.ac.uk, dyanne.cruickshank@uct.ac.za

Supporting information

Table S1. All variables investigated during the co-crystal screening studies*

API	Co-former	Ratio (API:co-former)	Solvent	Crystallisation temperature (°C)
Fenamic acid	Urea§	1:1	Methanol	4
Flufenamic acid	Oxalic acid	2:1	Isopropanol	18
Mefenamic acid	Isonicotinamide	1:2	Dimethylformamide	30
Tolfenamic acid	Nicotinic acid§		Ethanol	50
	4-aminobenzoic acid		Acetone	
	2-aminobenzoic acid		Tetrahydrofuran	
	Pyridoxine§			
	Isonicotinic acid hydrazide§			
	4,4'-bipiridyl			
	2,2'-bipridyl			
	2-aminopyridine			

§Classified as GRAS by the Select Committee on GRAS Substances (SCOGS)

***Note.** The crystallisations were prepared using the minimal solvent required for dissolution with the aid of a sonic bath (30 °C). All combinations of API, co-former and ratio stated in Table S1 were tested with one or more of the solvents listed dependant on solubility, so not all possible solvents were used for each combination. The maximum crystallisation temperature used was appropriate to the boiling point of the solvent used. Whilst co-crystals for all fenamic acid derivatives with 4,4'-bipyridine have been reported previously[1-3] these combinations have been included in this study but with a wider range of permutations than previously reported. Despite this extensive study only 4,4'-bipyridine yielded co-crystals.

Powder X-ray Diffraction Data

Fig. S1 PXRD patterns of the co-crystals obtained from evaporative methods and liquid assisted grinding (LAG).

FEN-BP

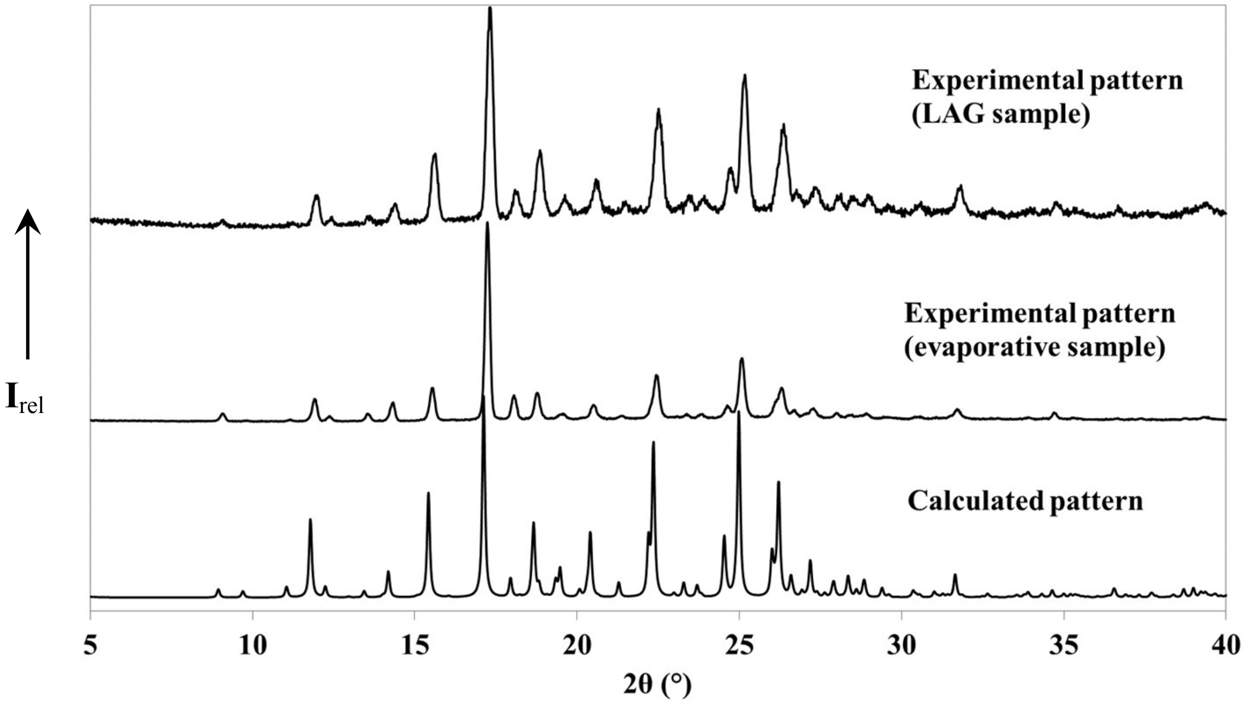

FLU-BP

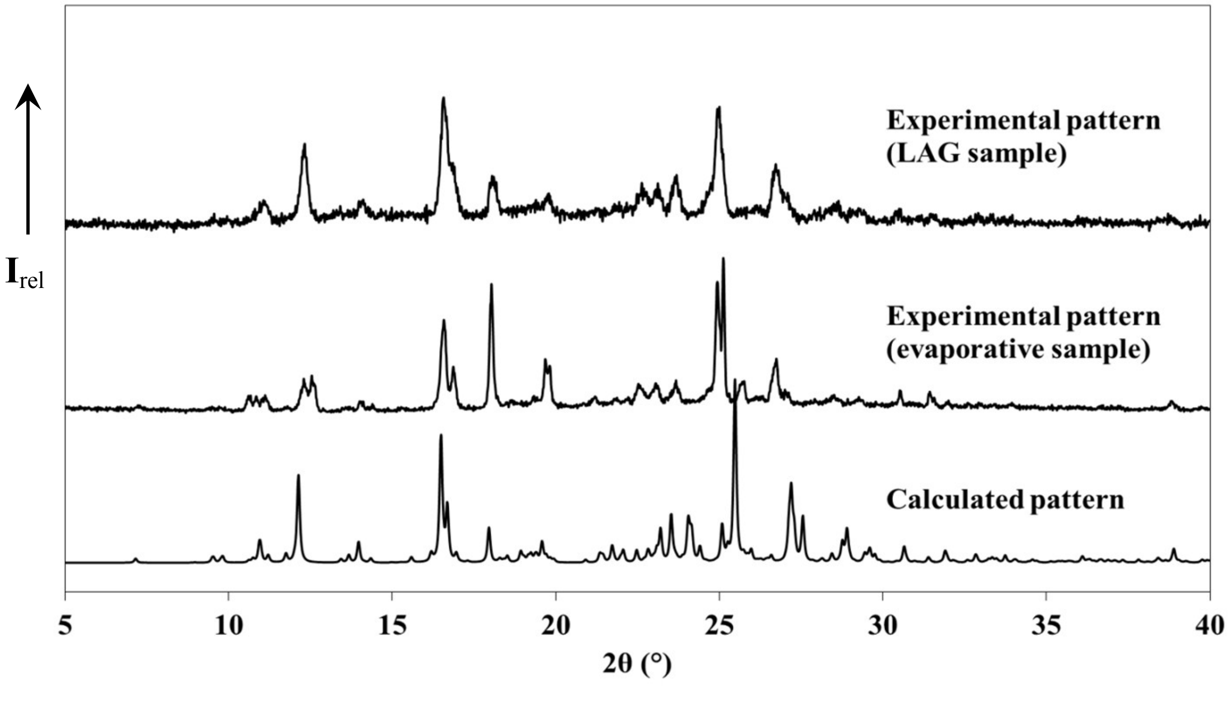

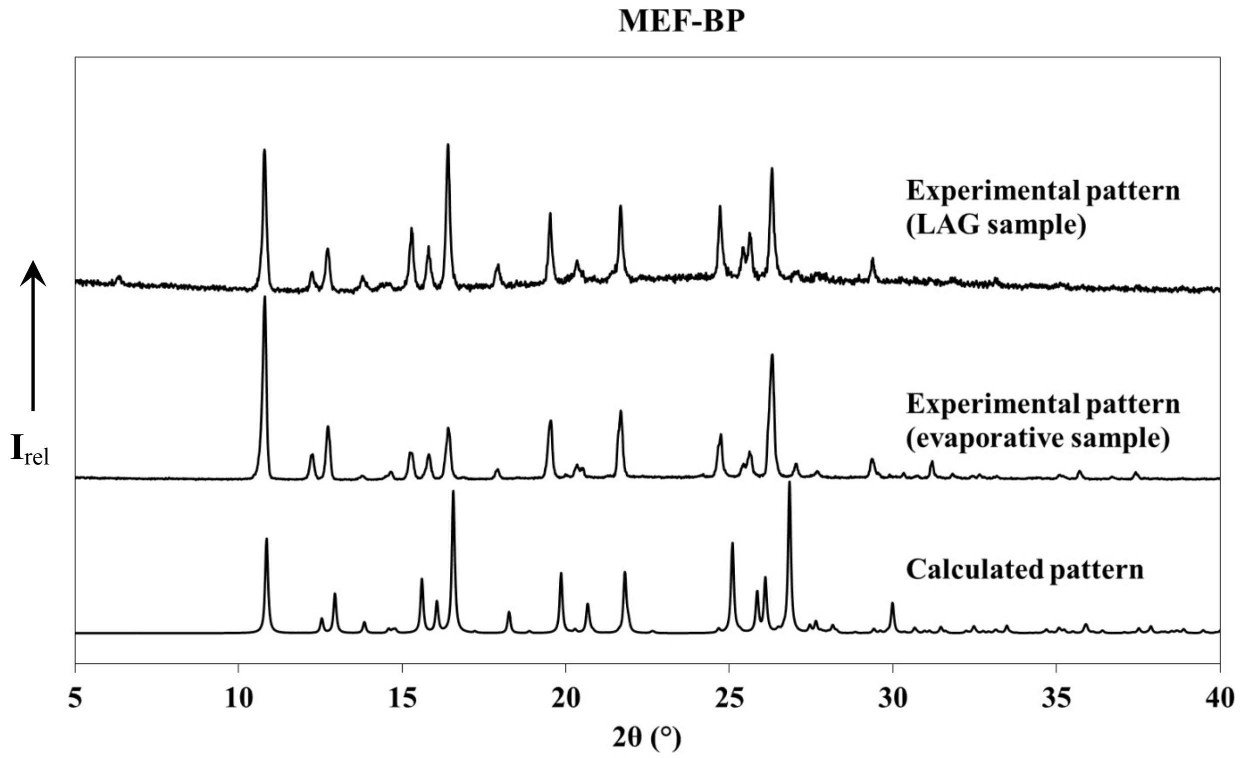
MEF-BP
Experimental pattern
(LAG sample)
Experimental pattern
(evaporative sample)
Calculated pattern
I_{rel}
5
10
15
20
25
30
35
40
2θ (°)

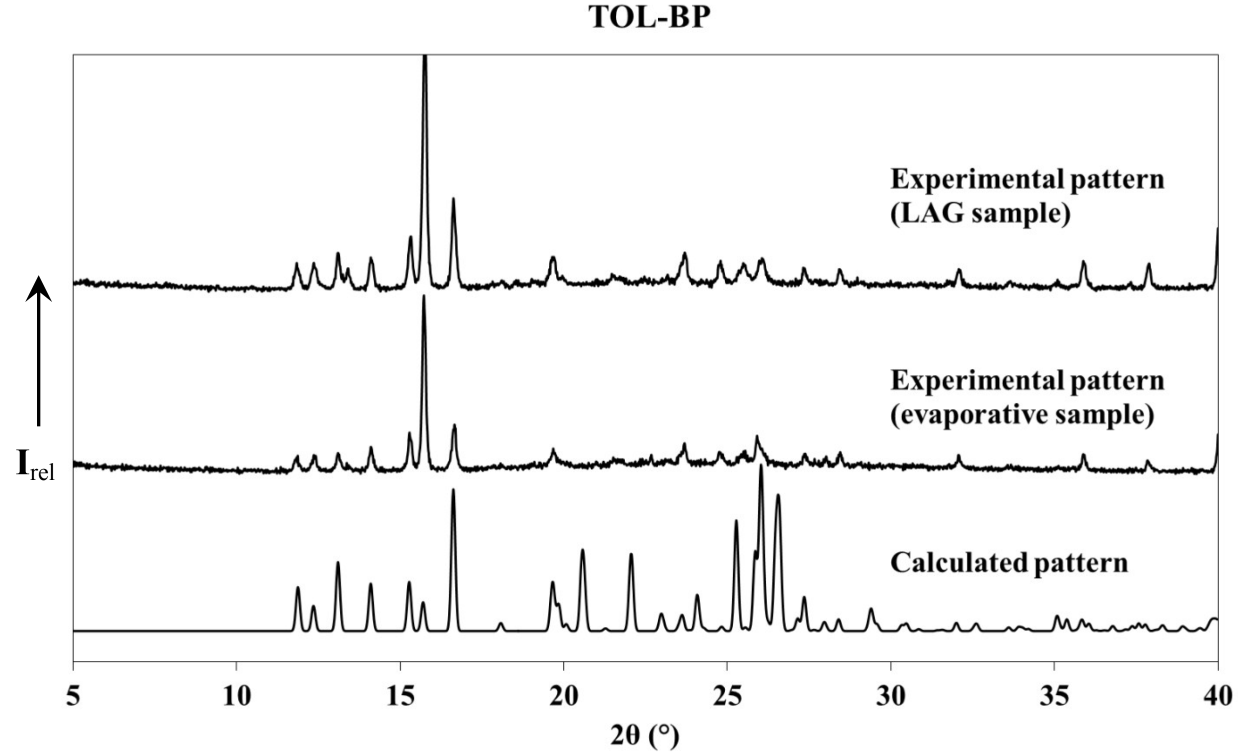
TOL-BP
Experimental pattern
(LAG sample)
Experimental pattern
(evaporative sample)
Calculated pattern
I_{rel}
5
10
15
20
25
30
35
40
2θ (°)

Crystallographic data

Table S2 Crystal data and structural refinement parameters for MEF-BP, TOL-BP and FLU-BP

Compound	MEF-BP	TOL-BP	FLU-BP
Formula unit	$2C_{15}H_{15}NO_2 \cdot C_{10}H_8N_2$	$2C_{14}H_{12}ClNO_2 \cdot C_{10}H_8N_2$	$2C_{14}H_{10}F_3NO_2 \cdot C_{10}H_8N_2$
M_r	319.37	339.79	1077.97
Crystal system	Triclinic	Monoclinic	Triclinic
Space group	$P\bar{1}$	$P2_1/c$	$P\bar{1}$
a/Å	7.3086(3)	4.7081(2)	9.8293(4)
b/Å	8.6692(4)	45.220(1)	10.3830(6)
c/Å	13.6320(5)	7.9188(3)	24.991(1)
α/°	106.135(4)	90	84.684(4)
β/°	99.428(4)	106.896(5)	81.333(4)
γ/°	98.758(4)	90	71.773(4)
V/Å^3	800.46(6)	1613.1(1)	2392.1(2)
No. of formula units per unit cell, Z	1	2	3
Crystal size/mm^3	0.20×0.15×0.10	0.20×0.18×0.08	0.13×0.11×0.08
ρ (calcd)/M g m^{-3}	1.325	1.399	1.497
μ/mm^{-1}	0.086	0.251	0.122
F(000)	338	708	1110
θ Range for data collection/°	2.89 - 29.64	3.01 - 26.37	2.80 - 25.35
Reflections collected	17917	11680	19891
No. of unique data	4011	3267	8741
[R(int)]	[0.0444]	[0.0387]	[0.0545]
No. of data with $I > 2\sigma(I)$	2899	2460	4684
Final $R(I > 2\sigma(I))$	0.0485	0.0520	0.0692
Final wR_2 (all data)	0.1137	0.1053	0.2055

Crystal structure description

The crystal structures of MEF-BP and TOL-BP (both form as 2:1 API:BP complexes)[1] contain the common acid-pyridine hydrogen bonded heterosynthon and intramolecular N-H···O hydrogen bond (Fig S2, Table S3) that has been seen previously in the other co-crystals of fenamic acid derivatives with BP.[2, 3] The contents of the asymmetric units of MEF-BP and TOL-BP, however, comprise one API molecule and half a BP molecule which is in contrast to the previously reported 2:1 co-crystals of FLU-BP and FEN-BP that have three and two API molecules in the asymmetric unit, respectively. The dihedral angles relating the mean planes of the phenyl rings for each API molecule in the FLU-BP and FEN-BP structures are considerably different, ranging from 49 to 70° for FEN-BP and from 41 to 47° for FLU-BP. The MEF-BP co-crystal displays the largest angle between the mean planes of the phenyl rings of 79.05(4)°.

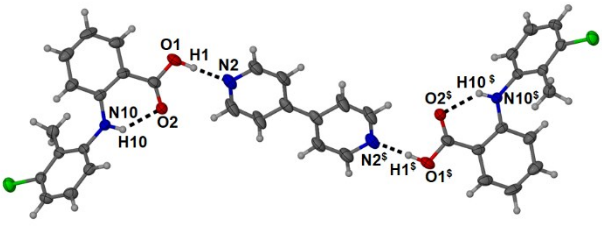

Fig. S2 The inter- and intramolecular hydrogen bonds of TOL-BP as a representative diagram for the two crystal structures discussed herein.

Table S3 Geometrical parameters for the significant hydrogen bonds of MEF-BP and TOL-BP

Hydrogen bond	*d*(H···A)/Å	*d*(D-H···A)/Å	∠(D-H···A)/°
MEF-BP			
O1-H1···N2[a]	1.72(2)	2.682(2)	178(2)
N10-H10···O2	1.94(2)	2.656(1)	137(2)
TOL-BP			
O1-H1···N2[b]	1.75(4)	2.674(4)	176(3)
N10-H10···O2	1.99(2)	2.659(3)	138(2)
C14-H14···Cl18[c]	2.81(2)	3.634(2)	146(2)

[a] x, 1+y, z; b1+x, y, z; c-1+x, 1/2-y, -1/2+z

The overall packing arrangements of MEF-BP and TOL-BP are significantly different from one another. The bipyridine molecule of MEF-BP lies co-planar with the benzoic acid group of mefenamic acid. These co-planar sections are positioned along the (2 -1 1) planes. The semi-perpendicular dimethyl phenyl rings form π-π interactions with their inversion-related counterparts (Fig S3) and two weak C-H···O interactions further stabilise the co-crystal and lock the conformation of MEF. The 4,4'-bipyridine molecule of TOL-BP is not co-planar to the benzoic acid group of tolfenamic acid (27(2)° angle between the mean planes; Fig S4.) which results in extended, twisted TOL-BP-TOL trimer units. The chlorine atoms form weak hydrogen bonds to a phenyl C-atom (C-H···Cl, 3.634(2) Å, 146(2)°). Further detailed structural descriptions and comparisons for MEF-BP, TOL-BP and other previously published fenamates with 4,4-bipyridine have been highlighted in the Surov et al paper.[1]

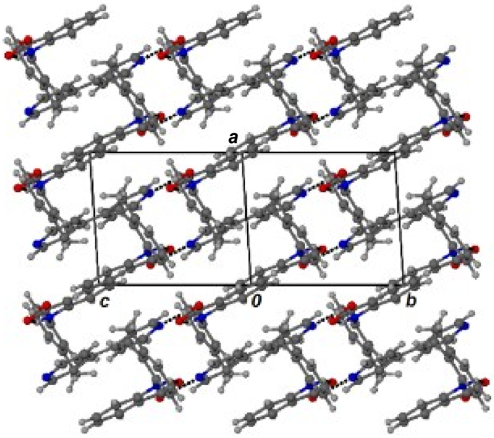

Fig. S3 The packing arrangement of the MEF-BP co-crystal as viewed along [011]

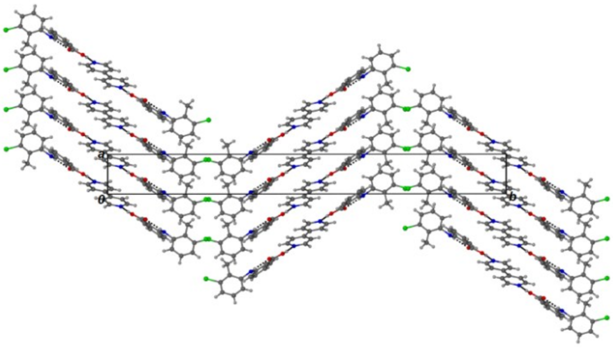

Fig. S4 A packing diagram of TOL-BP as viewed down the c-axis illustrating the non-planar relationship between the API and 4,4'-bipyridine molecules

Table S4. Melting points of the various polymorphs of mefenamic, tolfenamic and flufenamic [4-6] as well as their co-crystals with 4,4'-bipyridine. All temperatures are reported in °C

Polymorph	Mefenamic acid	Tolfenamic acid	Flufenamic acid
I	-†	213.10[5]	134.5[6]
II	229[4]	213.52[5]	129.6[6]
III	-‡	214.09[5]	127.4[6]
IV	-	206.78[5]	123.9[6]
V	-	215.17[5]	124.9[6]
VI	-	-	124.2[6]
VII	-	-	120.7[6]
BP Complex	163	156	128

† Converts to form II upon heating

‡Converts to form I at ambient temperature and form II upon heating

Fig. S5 FTIR spectra of the new fenamic acid derivative co-crystals and their individual components

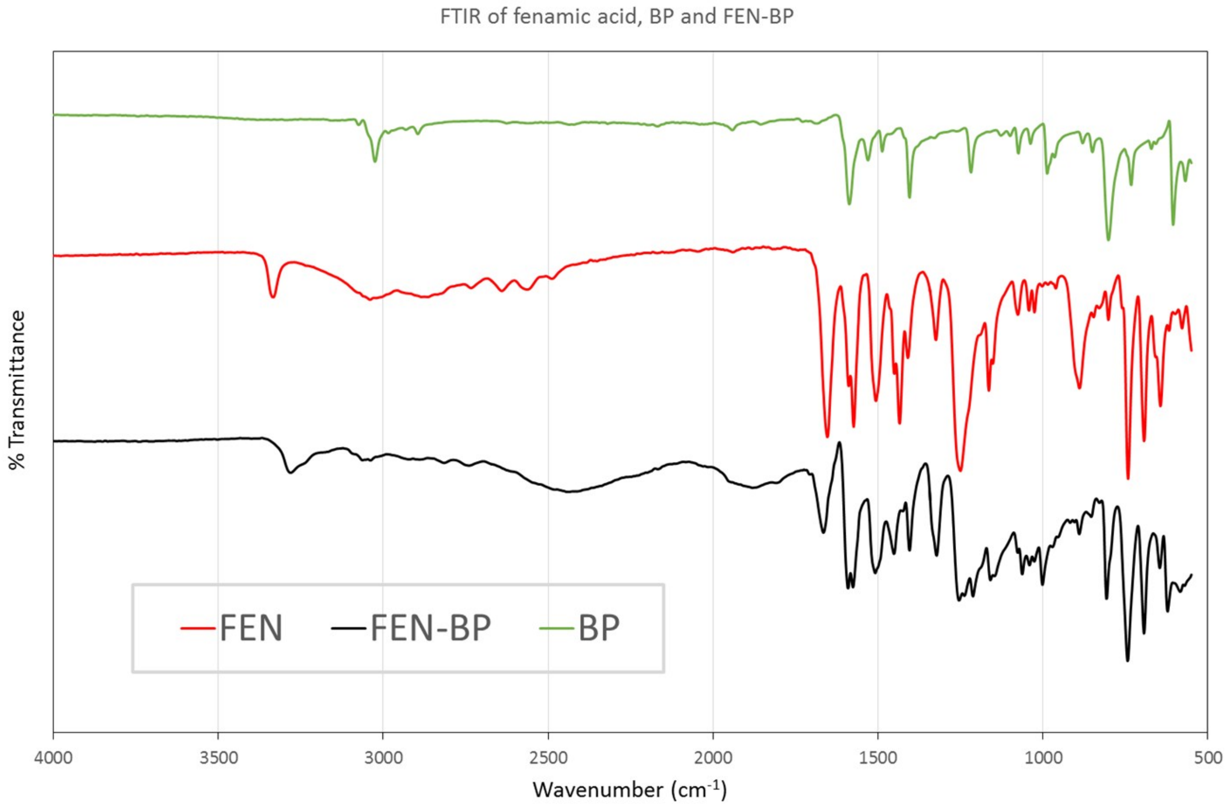

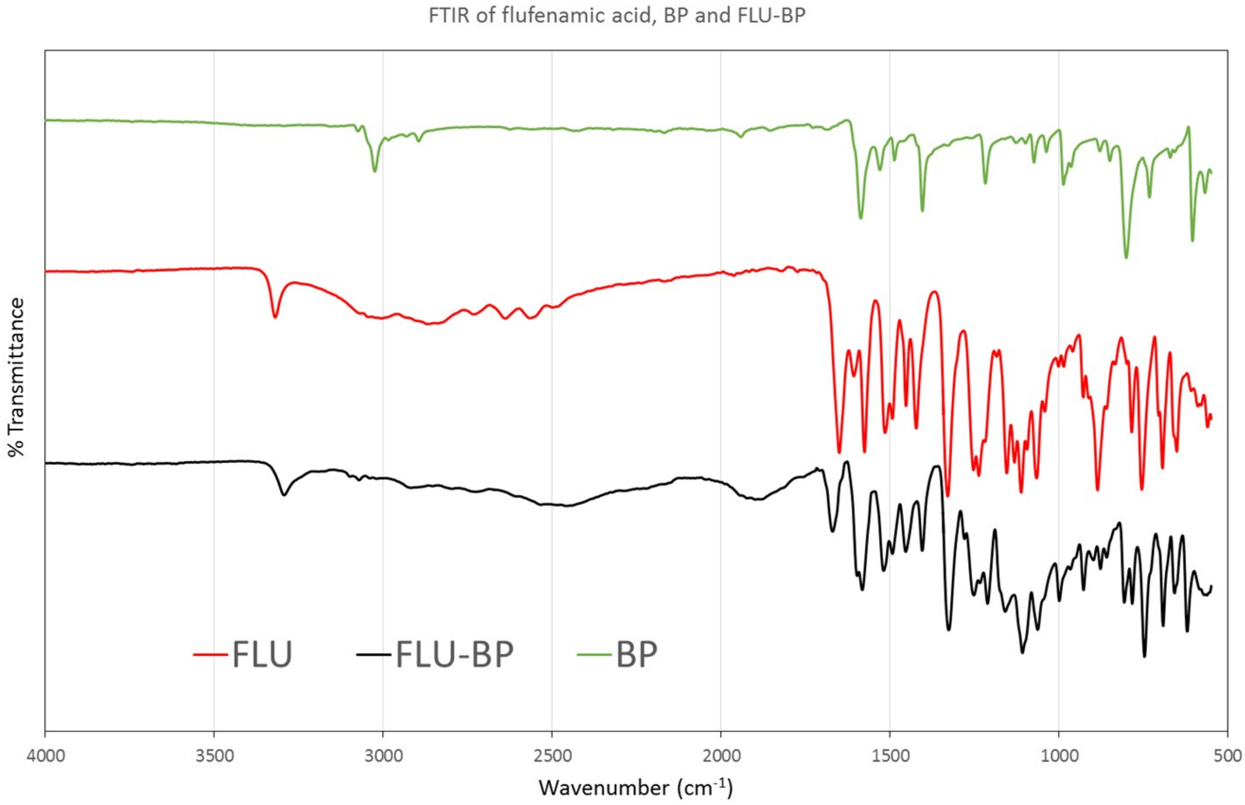

FTIR of mefenamic acid, BP and MEF-BP

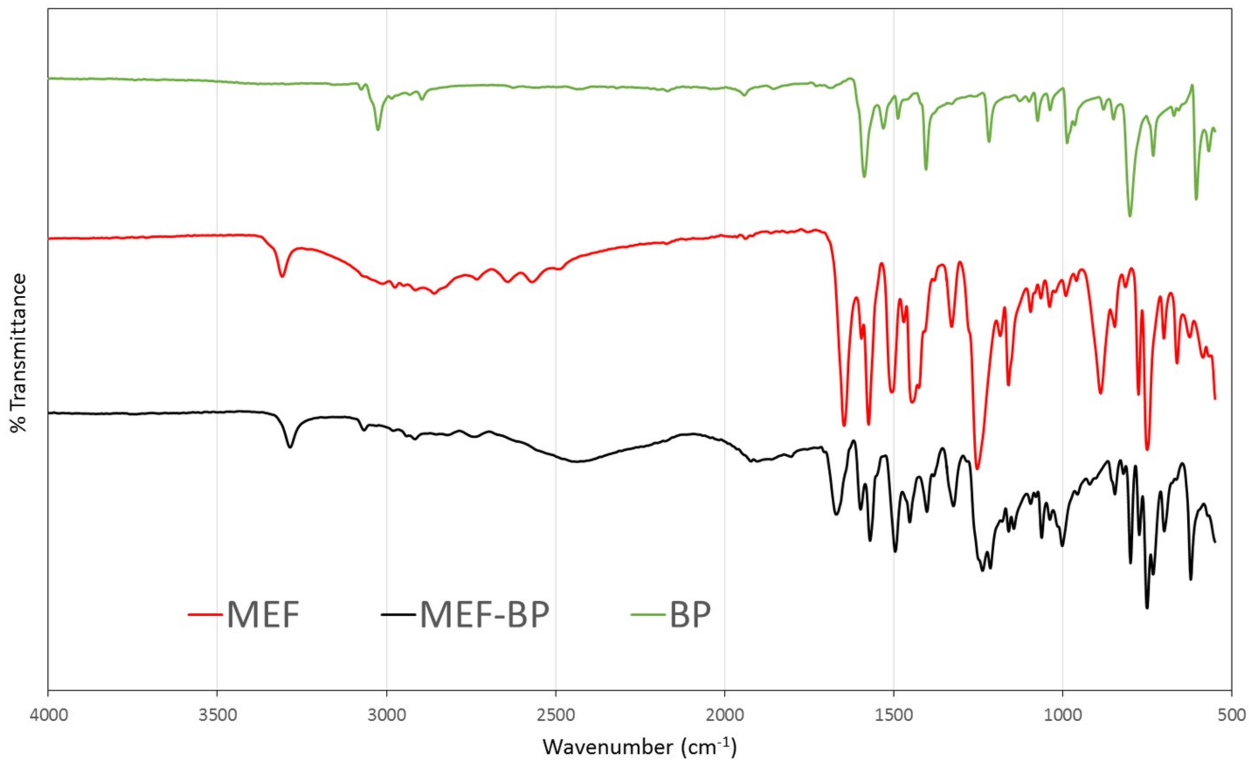

FTIR of tolfenamic acid polymorphs, BP and TOL-BP

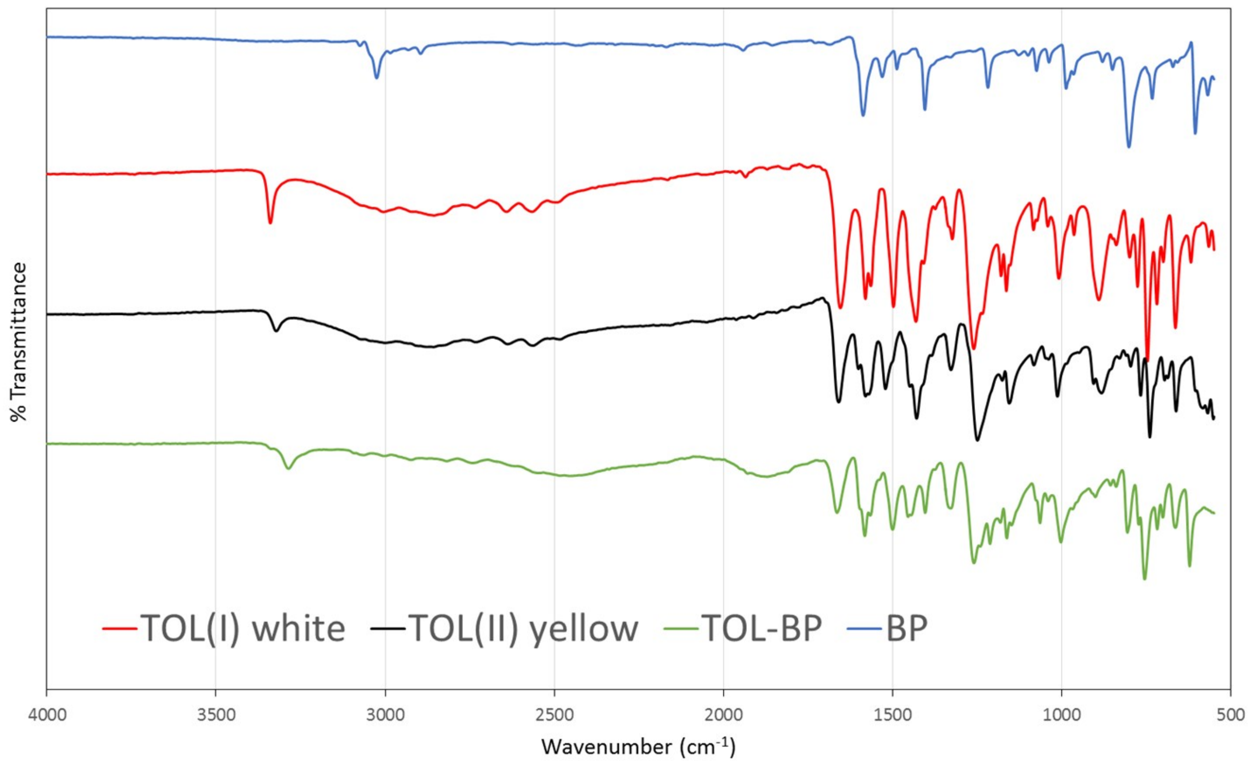

Fig. S6 PXRD patterns illustrating the stability of the fenamic acid derivatives in their native form and their respective co-crystals with 4,4’-bipyridine under moderate humidity conditions (24 °C and 45 % R.H.)

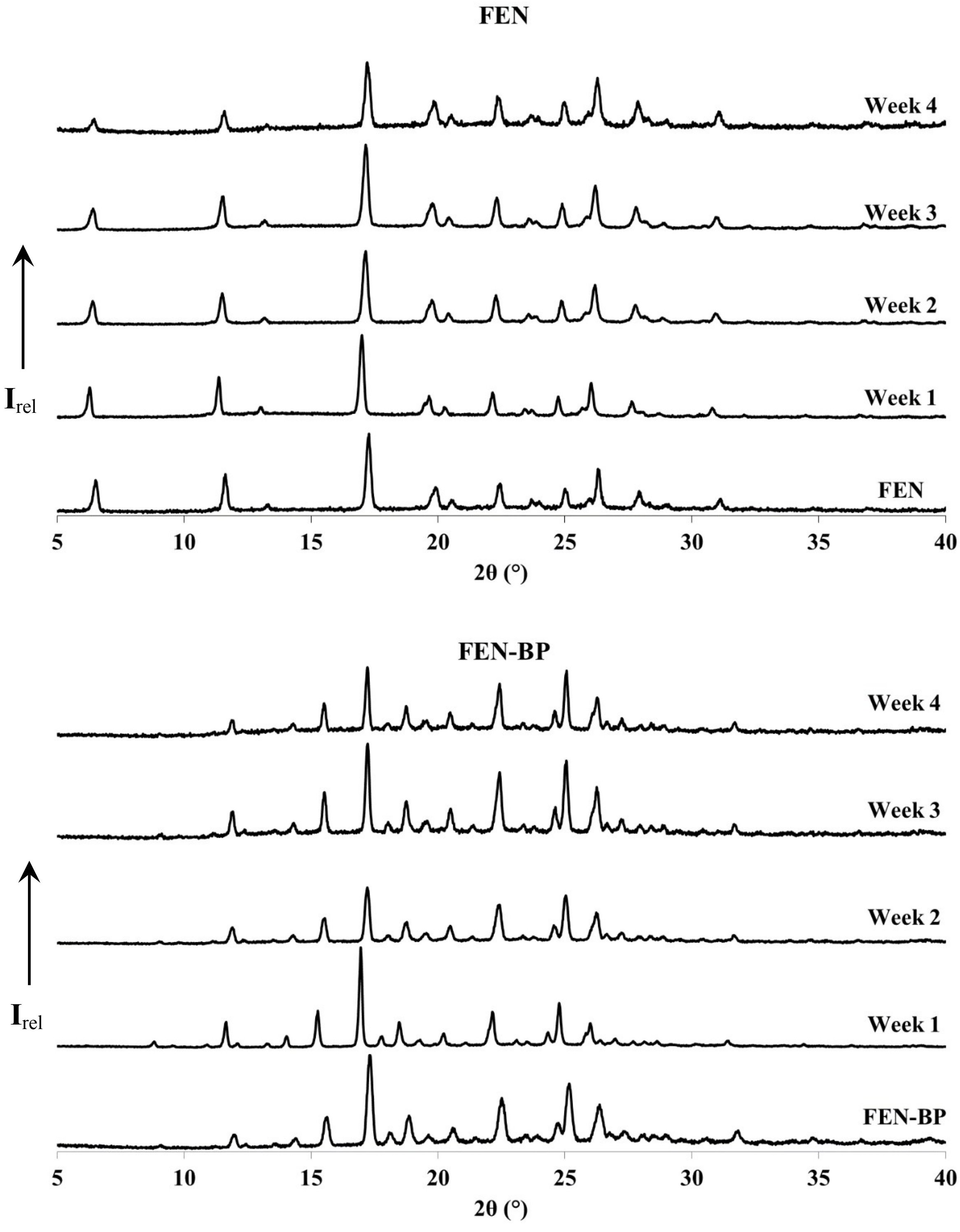

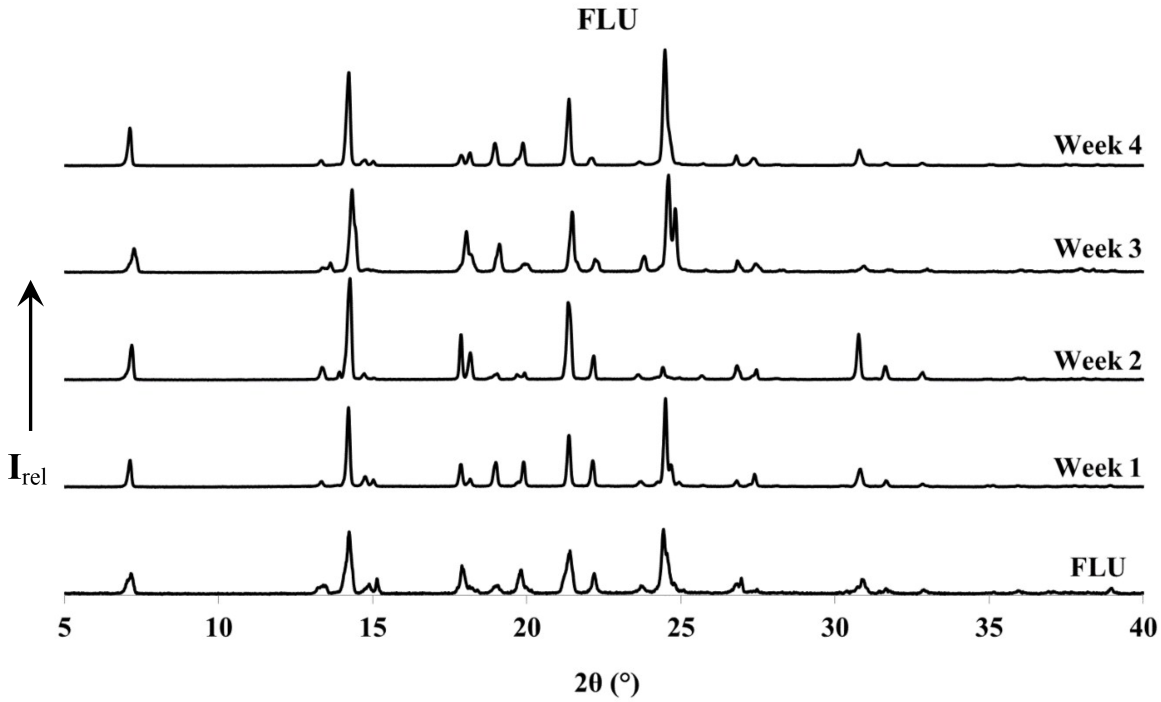
FLU
Week 4
Week 3
Week 2
Week 1
FLU
I_{rel}
5
10
15
20
25
30
35
40
2θ (°)

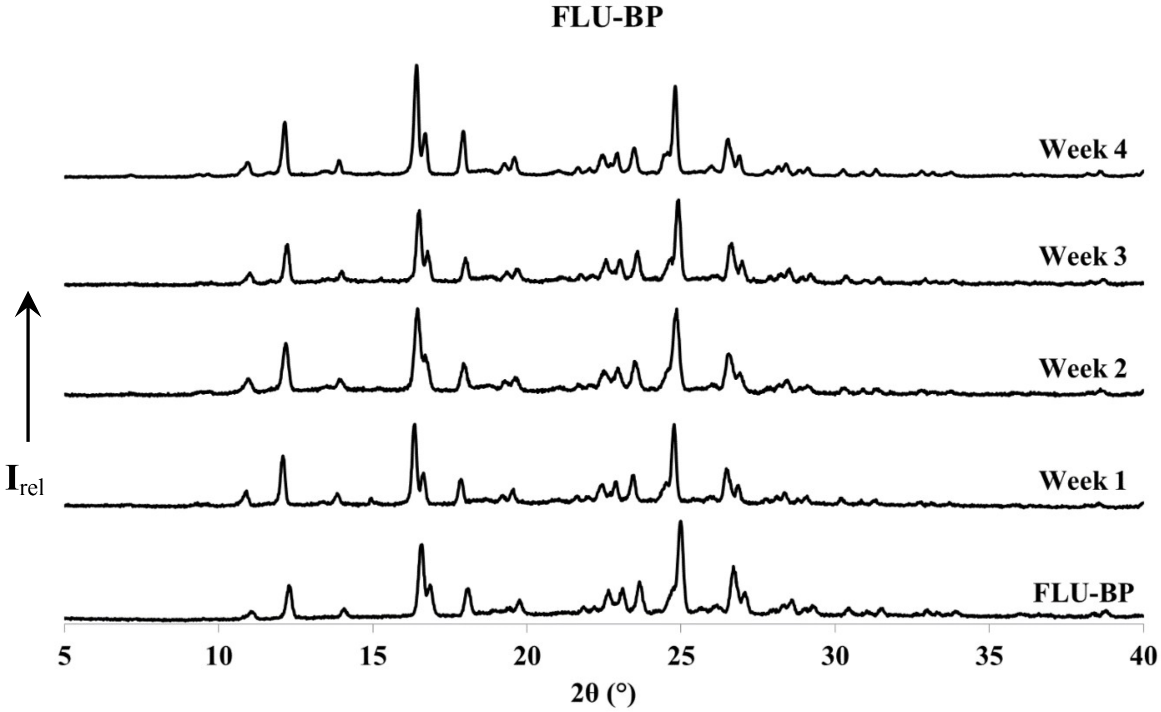
FLU-BP
Week 4
Week 3
Week 2
Week 1
FLU-BP
I_{rel}
5
10
15
20
25
30
35
40
2θ (°)

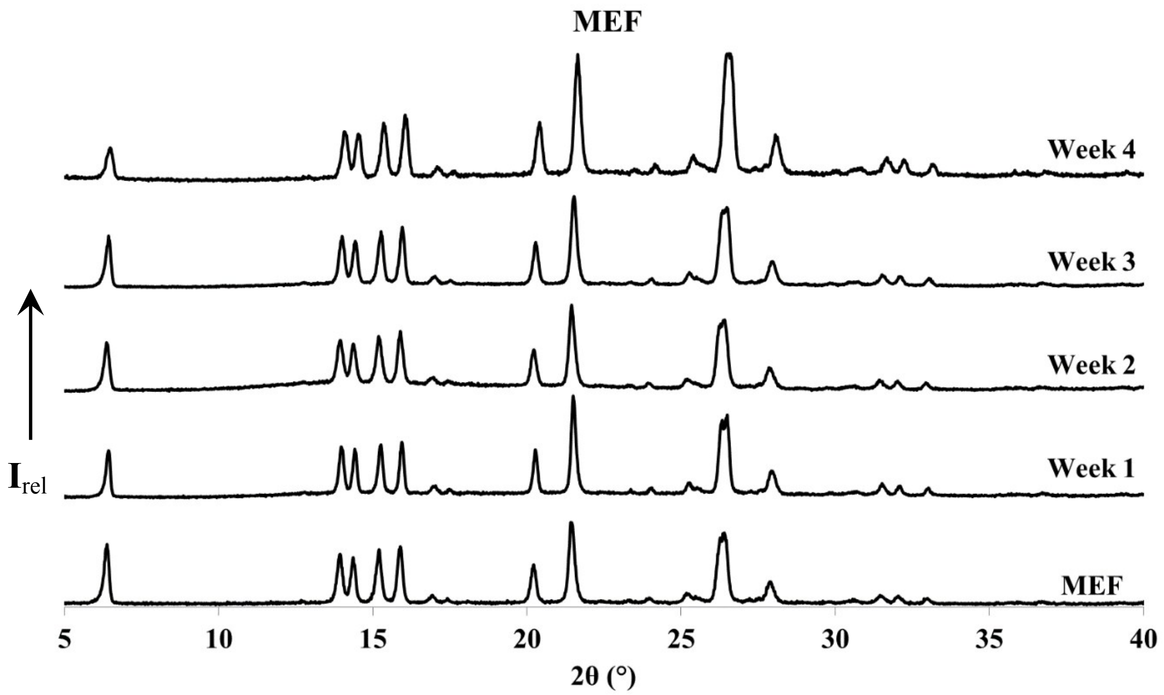
MEF
Week 4
Week 3
Week 2
Week 1
MEF
I_{rel}
5
10
15
20
25
30
35
40
2θ (°)

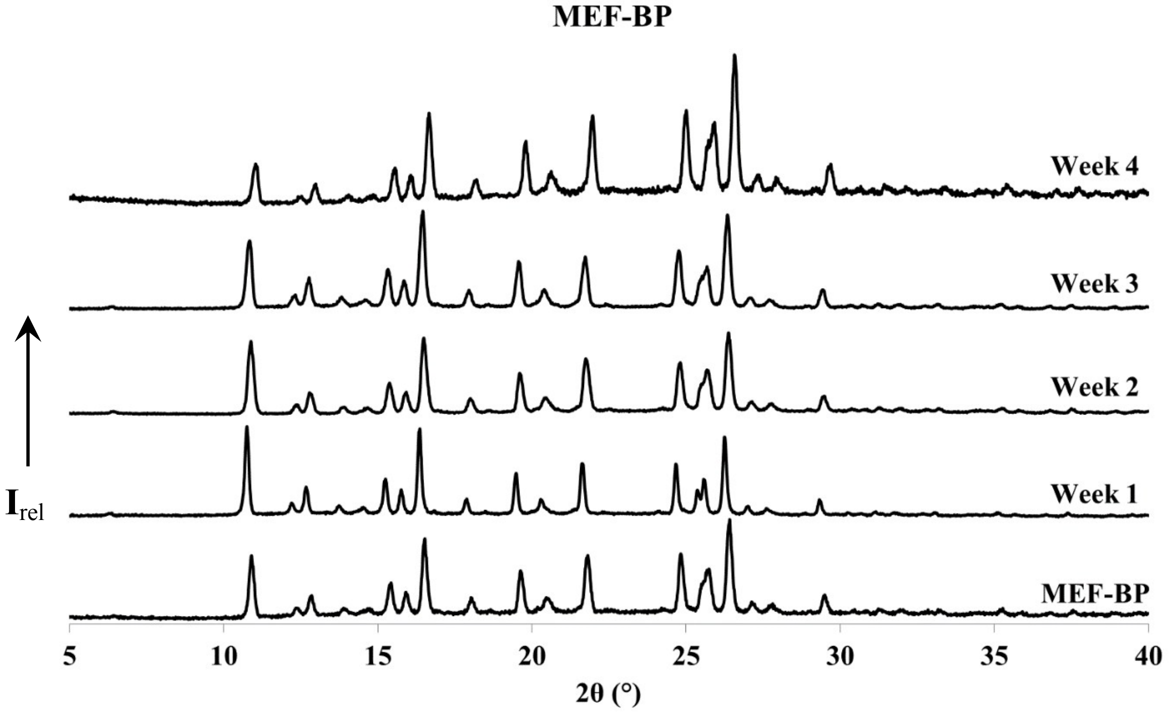
MEF-BP
Week 4
Week 3
Week 2
Week 1
MEF-BP
I_{rel}
5
10
15
20
25
30
35
40
2θ (°)

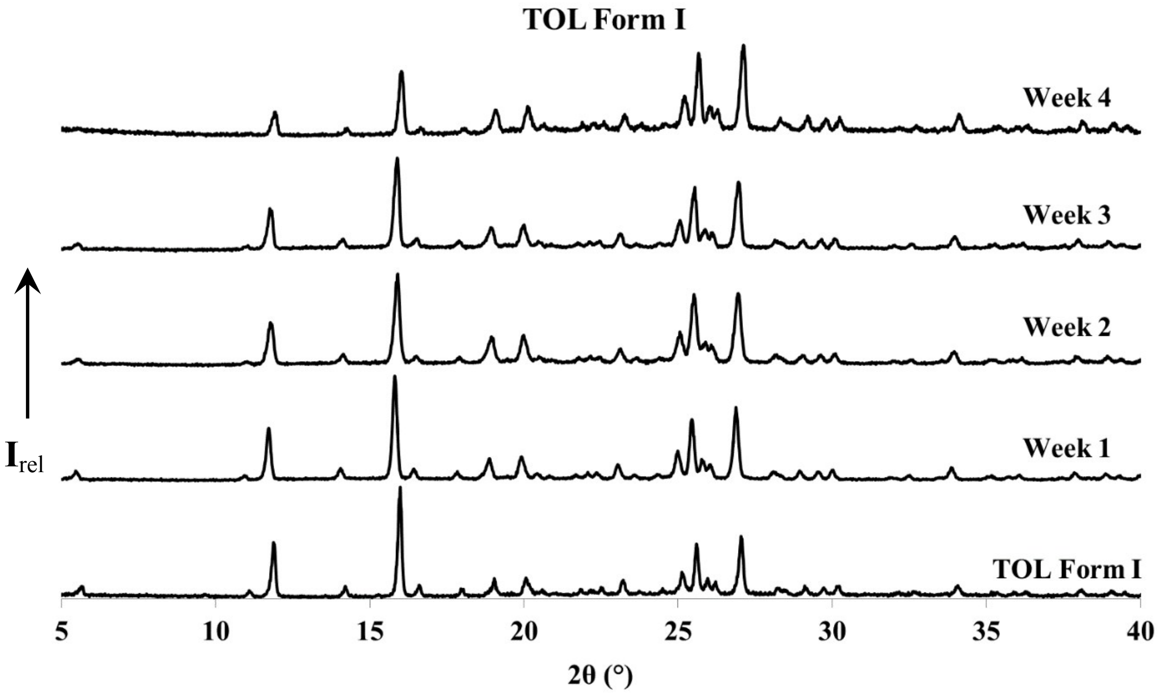
TOL Form I
Week 4
Week 3
Week 2
Week 1
TOL Form I
I$_{rel}$
5
10
15
20
25
30
35
40
2θ (°)

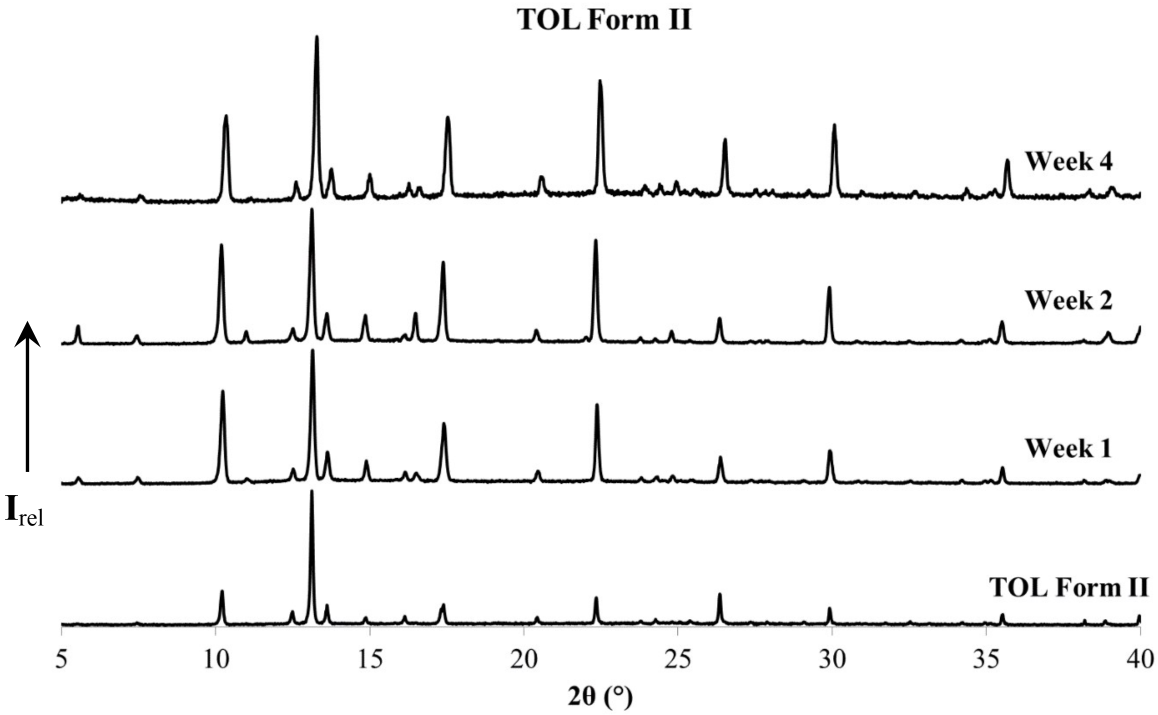
TOL Form II
Week 4
Week 2
Week 1
TOL Form II
I$_{rel}$
5
10
15
20
25
30
35
40
2θ (°)

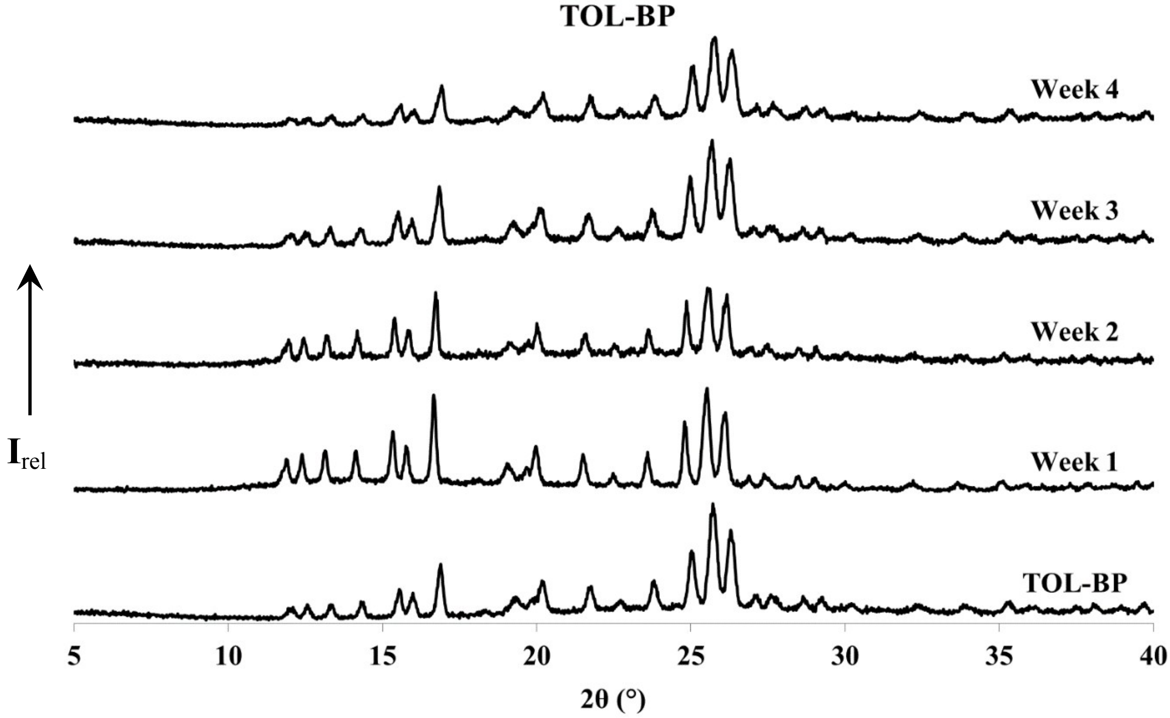

Fig. S7 PXRD patterns illustrating the stability of the fenamic acid co-crystals with 4,4’-bipyridine under harsh humidity conditions (45 °C and 80 % R.H.)

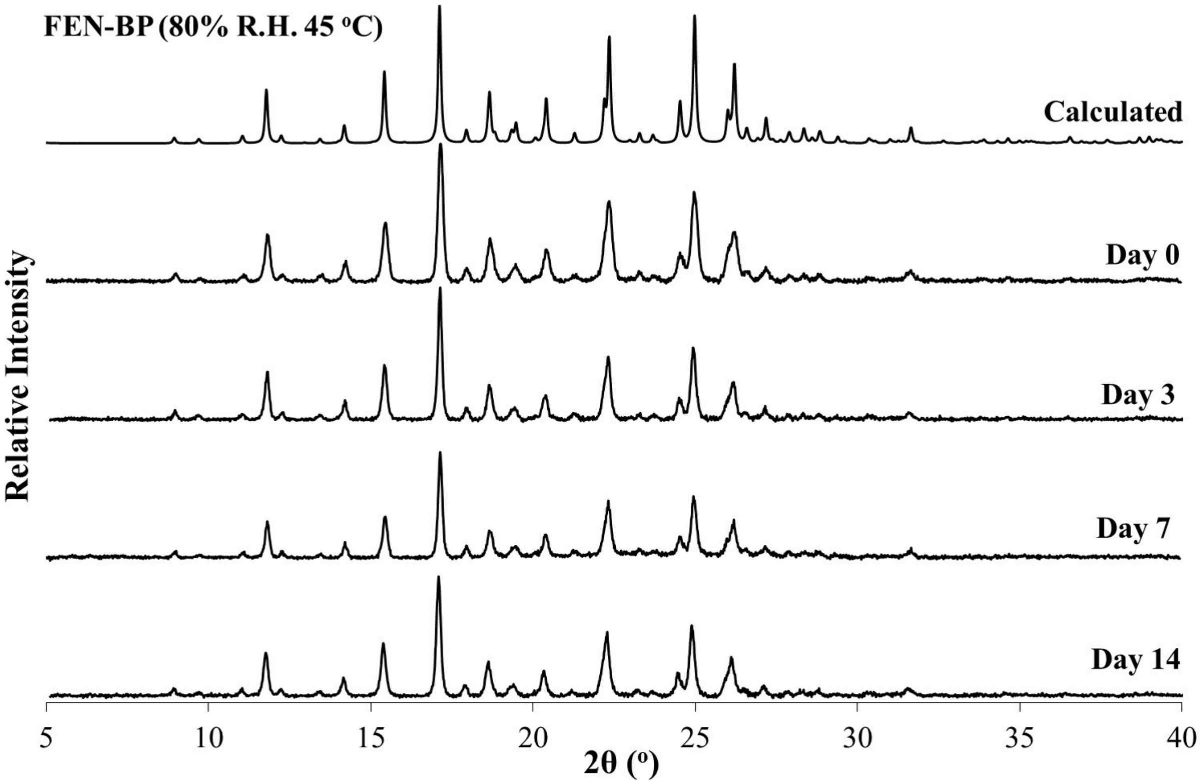

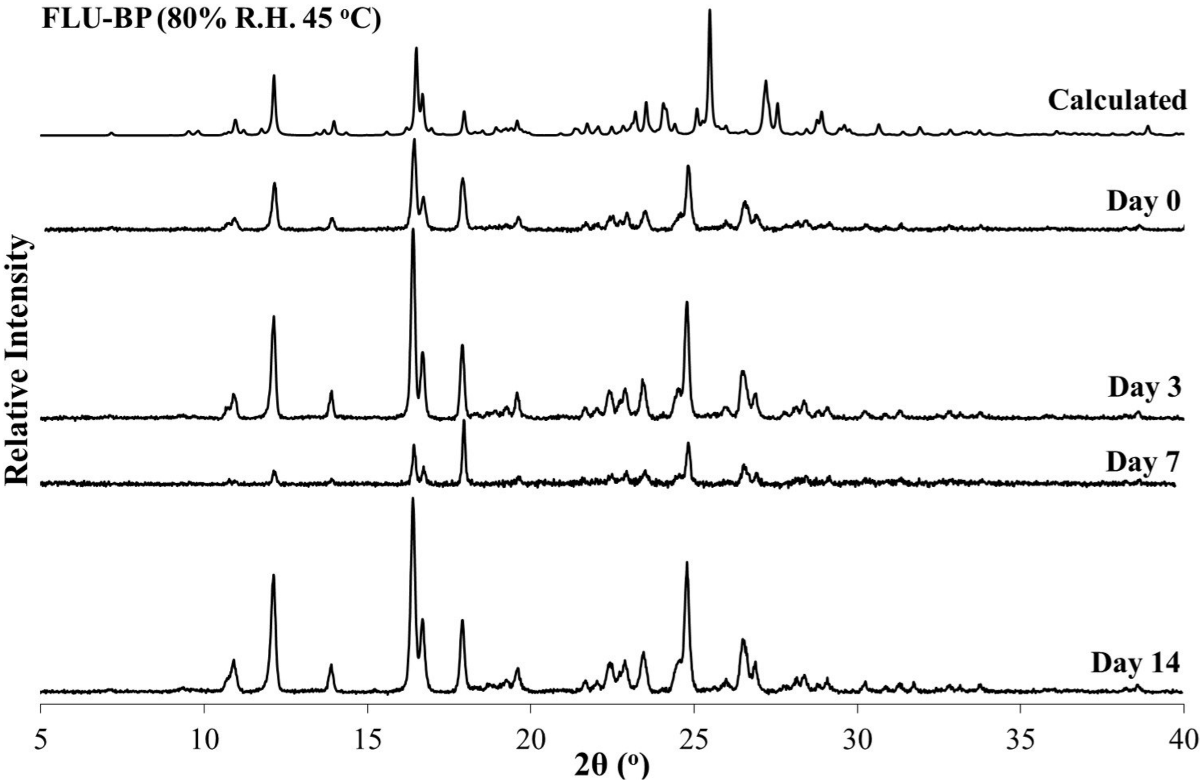
FLU-BP (80% R.H. 45 ºC)
Calculated
Day 0
Day 3
Day 7
Day 14
Relative Intensity
5
10
15
20
25
30
35
40
2θ (º)

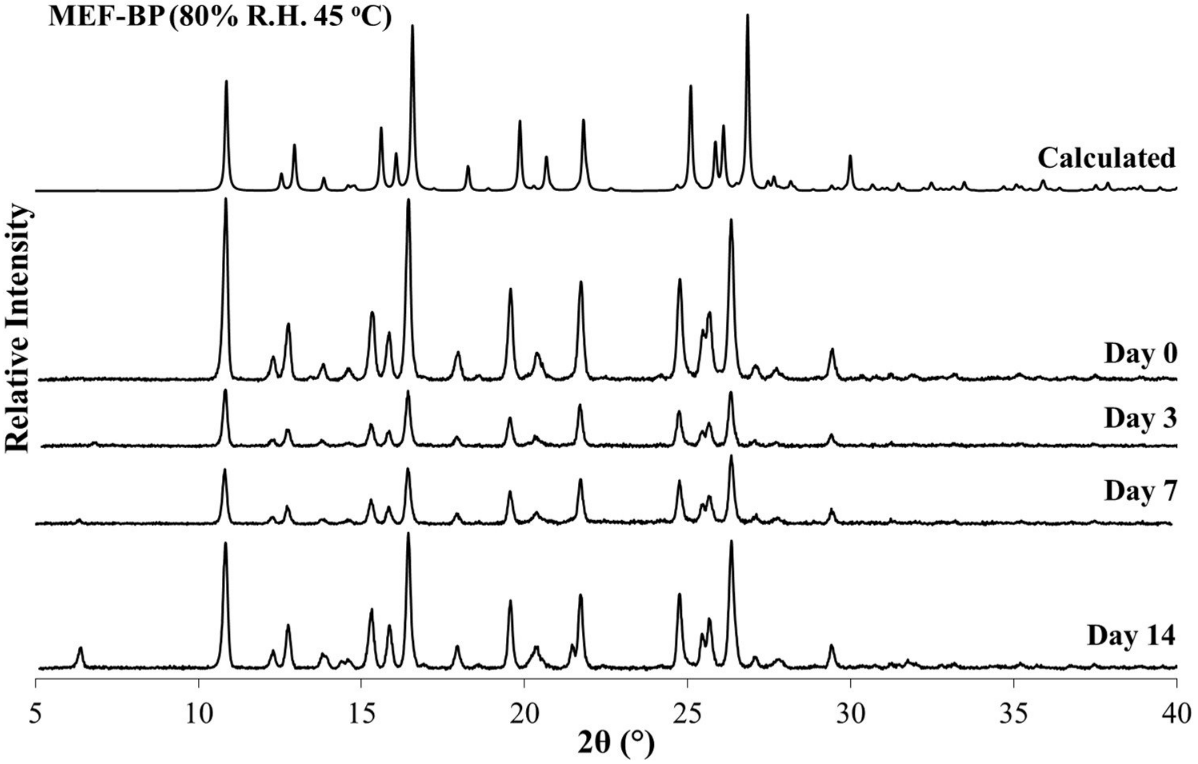
MEF-BP (80% R.H. 45 ºC)
Calculated
Day 0
Day 3
Day 7
Day 14
Relative Intensity
5
10
15
20
25
30
35
40
2θ (°)

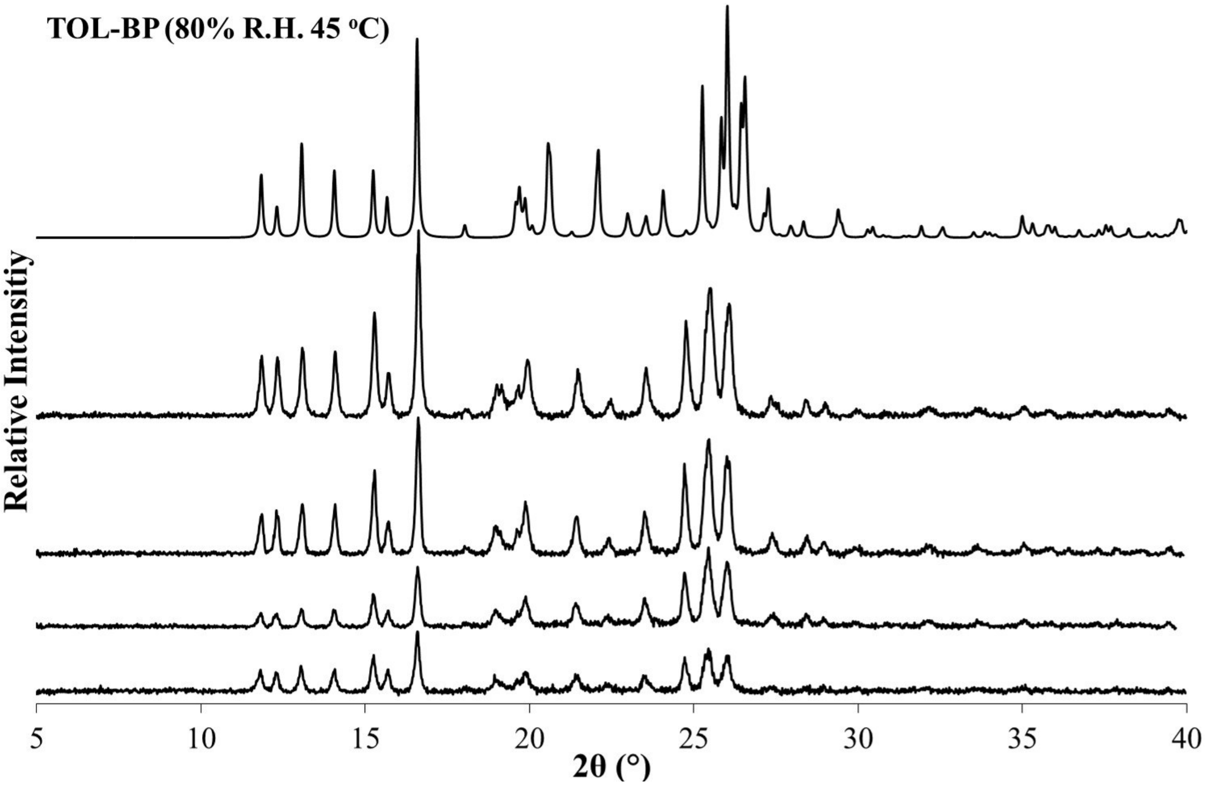

***Note.** Shifts in the calculated patterns for FLU-BP, MEF-BP and TOL-BP are due to the low temeperatures (150 K) at which the single crystal X-ray data was collected.

References

1 A. O. Surov, A. A. Simagina, N. G. Manin, L. G. Kuzmina, A. V. Churakov and G. L. Perlovich, *Cryst. Growth Des.*, 2014, 10.1021/cg5012633.

2 S. Kumaresan, P. G. Seethalakshmi, P. Kumaradhas and B. Devipriya. *J. Mol. Struct.* 2013, **1032**, 169-175.

3 S. Aitipamula, A. B. H. Wong, P. S. Chow and R. B. H. Tan, *CrystEngComm*, 2014, **16**, 5793-5801.

4 S. SeethaLekshmi and T. N. Guru Row, *Cryst. Growth Des.*, 2012, **12**, 4283-4289.

5 V. López-Mejías, J. W. Kampf and A. J. Matzger, *J. Am. Chem. Soc.*, 2009, **131**, 4554-4555.

6 V. López-Mejías, J. W. Kampf and A. J. Matzger, *J. Am. Chem. Soc.*, 2012, **134**, 9872-9875.